A Mg-Zn-Y-Zr icosahedral quasi-crystal containing linear phason strain

1994 J. Phys.: Condens. Matter 6 7329

(http://iopscience.iop.org/0953-8984/6/36/015)

J. Phys.: Condens. Matter 6 (1994) 7329–7334. Printed in the UK

A Mg–Zn–Y–Zr icosahedral quasi-crystal containing linear phason strain

Dongshan Zhao†, Yali Tang‡, Zhiping Luo§, Renhui Wang‖, Ningfu Shen‡ and Shaoqing Zhang§

† Department of Mathematics and Mechanics, Zhengzhou Institute of Technology, Zhengzhou 450002, People's Republic of China

‡ Research Center for Materials, Zhengzhou Institute of Technology, Zhengzhou 450002, People's Republic of China

§ Institute of Aeronautical Materials, Beijing 100095, People's Republic of China

‖ Department of Physics, Wuhan University, Wuhan 430072, People's Republic of China

Received 23 December 1993, in final form 5 May 1994

Abstract. Distorted electron diffraction patterns from a Mg–Zn–Y–Zr icosahedral quasi-crystal have been observed and interpreted by introducing a special linear phason strain.

1. Introduction

Since the discovery of the icosahedral quasi-crystal (IQC) in a rapidly solidified Al–Mn alloy [1], other quasi-crystals (QC)s have been reported soon, such as the decagonal [2], dodecagonal [3], octagonal [4] and cubic [5] QCs. In addition to QCs first found in rapidly solidified alloys, many stable IQCs and/or decagonal quasi-crystals have been identified in Al–Cu–Li [6–8], Al–Cu–Fe [9], Al–Cu–Co [10, 11], Al–Cu–Mn [12], Al–Mn–Pd [13], Al–Pd–(Fe, Ru or Os) [14] and Ga–Mg–Zn [15] systems by conventional solidification. Besides perfect QCs there are also QCs containing phason strains demonstrated by the shift in the diffraction spots of the electron diffraction patterns (EDPs) [16–18]. When the phason strain parameter reaches certain values, the phason-strained QCs become crystalline approximants [17, 18].

Recently, we have reported a new kind stable IQC phase in as-cast Mg–Zn–RE alloys (RE represents high-grade Y or mischmetals containing Y, Nd, Gd, Dy, La, Pr, Tb and Ce) [19]. In this paper we shall present our recent results on the existence of phason-strained Mg–Zn–Y–Zr IQC phases.

2. Experimental method and results

The experimental materials were melted in an electric furnace under an inert atmosphere and slowly cooled in air. Their compositions are 4.77–6.3 wt% Zn, 0.52–1.72 wt% RE (as indicated above), 0.35–0.72 wt% Zr and balance Mg. The specimen was obtained directly from the cast ingot. The foils for transmission electron microscopy (TEM) were prepared by electropolishing and ion beam thinning and then examined in a JEM-2000FX electron microscope equipped with a LINK AN-10000 energy-dispersive x-ray spectrometer. In these cast alloys, compounds are distributed along the grain boundaries as shown in figure 1(a). In

0953-8984/94/367329+06$19.50

these compounds, many IQC grains exist. The energy-dispersive spectroscopy (EDS) analysis (figure 1(b)) of the IQC phase reveals Mg, Zn, Y, Cu and Zr peaks; the Cu peaks are from the specimen mesh and are not considered in the quantitative analysis. By this means the average composition of the IQC phase is determined to be $Mg_{16}Zn_{68}Y_8Zr_5$.

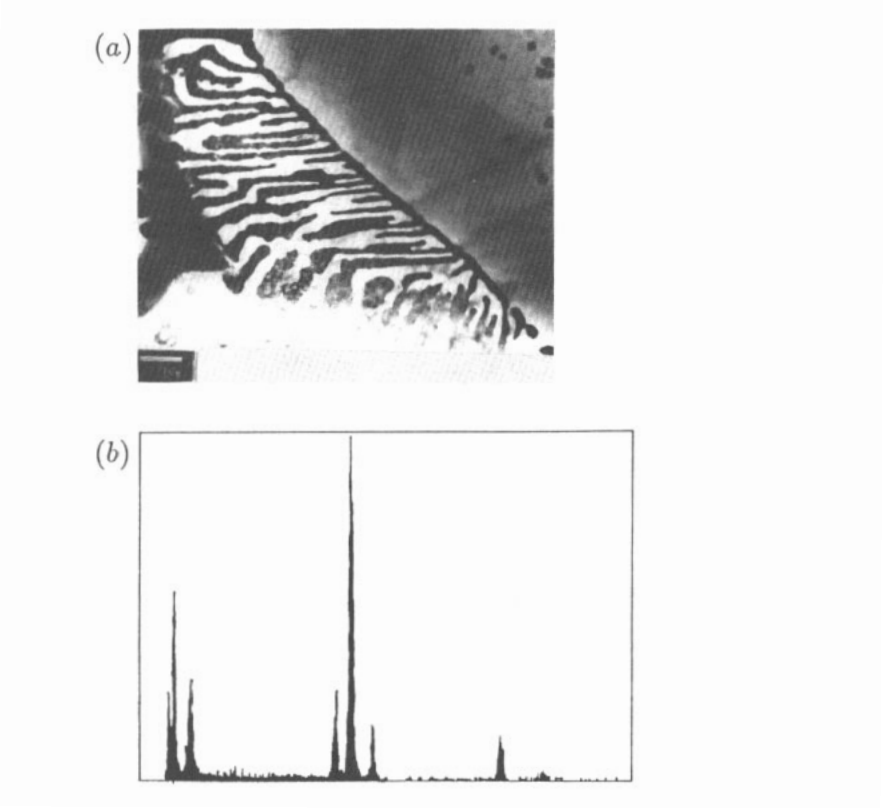

Figure 1. IQC grains in Mg–Zn–Y–Zr alloy; (*a*) morphology; (*b*) EDS from the Mg–Zn–Y–Zr IQC.

Almost all the IQC grains are imperfect indicated by their distorted EDPs. The region circled in figure 1(*a*) gives distorted EDPs as shown in figure 2(*a*) and figure 3(*a*) which are along the twofold and fivefold axes, respectively. The diffraction spots slightly deviate from their standard positions, with the weaker spots showing larger deviations. For instance, spot A is clearly displaced downwards, and spot B less obviously upwards, while the displacement of spot C is almost invisible. Clearly, the deviation direction of all the spots is along the vertical direction, which coincides with one of the twofold axes of the IQC. These facts are very similar to those for the Al–Cu–Mg IQC phase observed by Li *et al* [17]. In addition, we examined other IQC grains by selected-area electron diffraction and obtained different twofold EDPs (shown in figure 4) with respect to figure 2(*a*). Figure 4 reveals more strong diffraction spots than figure 2(*a*) along the fivefold directions (indicated by arrows in figure 4 and figure 2(*a*)). Ebalard and Spaepen [20] first studied the EDPs with similar characteristics in the $Al_{65}Cu_{20}Fe_{15}$ IQC system. They explained this by ascribing a face-centred icosahedral (FCI) structure to the $Al_{65}Cu_{20}Fe_{15}$ IQC in contrast with the simple icosahedral (SI) structure of an IQC such as Al_4Mn and $Al_{76}Si_4Mn_{20}$. The EDP in figure 4 is

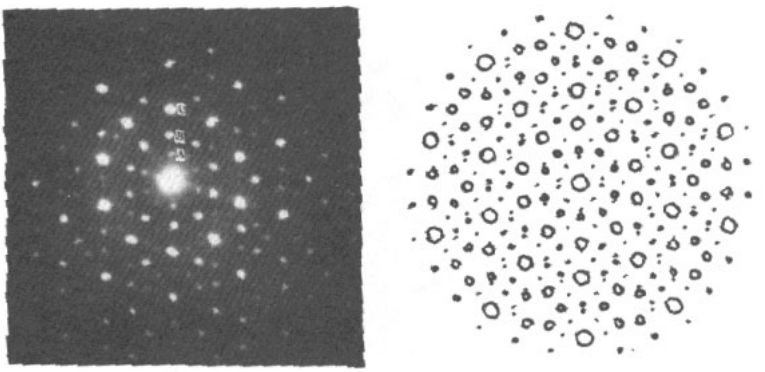

(a) (b)

Figure 2. EDPs along the twofold axis of the Mg–Zn–Y–Zr IQC: (*a*) experimental; (*b*) simulated with a linear phason strain along the vertical direction ($m = -0.10$).

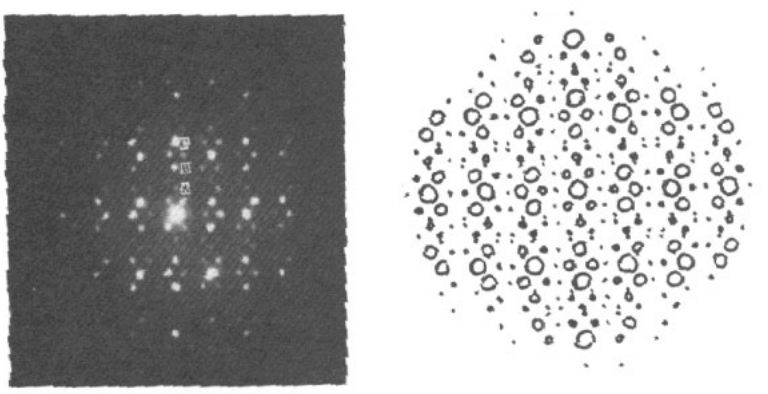

(a) (b)

Figure 3. EDPs along the fivefold axis of the Mg–Zn–Y–Zr IQC: (*a*) experimental; (*b*) simulated with a linear phason strain along the vertical direction ($m = -0.10$).

distorted too, indicated by the fact that the spots along fivefold direction are zigzag, with spots a and b showing larger deviations.

3. Computer simulation of the distorted electron diffraction patterns of simple icosahedral structure

According to Kramer [21] and Elser [22], the three-dimensional (3D) Penrose tiling of the IQC with SI structure may be constructed as a projection from a subset of a six-dimensional (6D) hypercubic lattice with basis vectors e^i ($i = 1, 2, \ldots, 6$). The projected basis vectors $e^i_{\parallel}$ of these e^i in a special 3D physical subspace $E^3_{\parallel}$ coincide with the six vertices of the icosahedron as shown in figure 5(*a*). The projected basis vectors $e^i_{\perp}$ in the 3D complementary

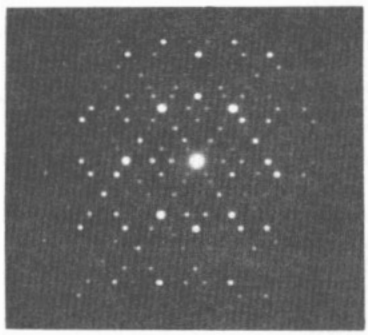

Figure 4. EDPs along the twofold axis of the Mg–Zn–Y–Zr IQC with the FCI structure.

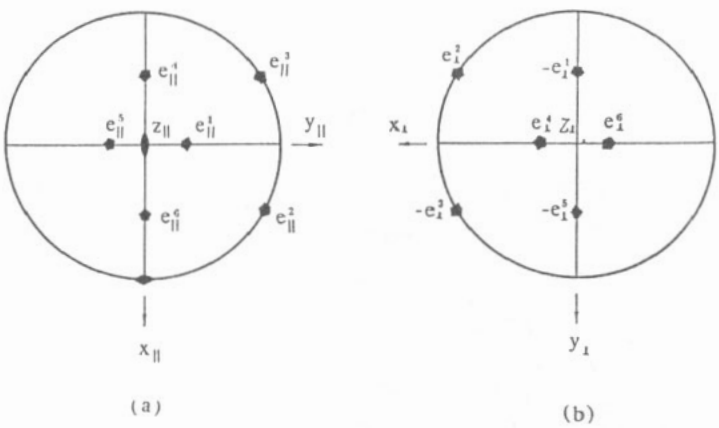

Figure 5. The stereographic projection of the projected basis vectors: (*a*) $e_{\parallel}^{i}$ in $E_{\parallel}^{3}$; (*b*) $e_{\perp}^{i}$ in $E_{\perp}^{3}$.

subspace $E_{\perp}^{3}$ are shown in figure 5(*b*). In the present work we apply the same method to calculate the diffraction intensities of the IQC phase as used by Zhao *et al* [23]. They assumed a simple lattice model in which the same atom with a unit atomic scattering factor $f(g_{\parallel}) = 1$ is placed at every quasi-lattice point.

According to Lubensky *et al* [16], a linear phason strain will cause each Bragg peak to shift from the position given by the reciprocal vector $g_{\parallel}$ of an unstrained IQC phase to $g'_{\parallel} = g_{\parallel} + \Delta g_{\parallel}$ with

$$\begin{bmatrix} \Delta g_{\parallel x} \\ \Delta g_{\parallel y} \\ \Delta g_{\parallel z} \end{bmatrix} = -\mathbf{M} \begin{bmatrix} g_{\perp x} \\ g_{\perp y} \\ g_{\perp z} \end{bmatrix}$$

where **M** is a 3 × 3 matrix which represents the phason shear field, and to keep its corresponding perpendicular component $g_{\perp}$ unchanged. According to Li and co-workers [17, 18], we choose

$$\mathbf{M} = \begin{bmatrix} 0 & 0 & 0 \\ 0 & 0 & 0 \\ 0 & 0 & m \end{bmatrix}.$$

This matrix corresponds to the phason strain direction along the $Z_\perp$ axis which induces a shift in the Bragg peaks along the $Z_\parallel$ axis parallel to a twofold axis of the IQC phase (see figure 5). Hence, the zone axes of the EDPs in figures 2 and 3 are along the positive $X_\parallel$ axis and the basis vector $e_\parallel^2$, respectively (see figure 5(*a*)).

Since the scattering amplitude $S(g_\parallel)$ [23] depends mainly on the perpendicular component $g_\perp$) which remains unchanged when the phason parameter m is varied, the diffraction intensity is independent of the m-value. Of course, exceptions may happen when several reciprocal points in the 6D hyperspace are projected into the same reciprocal point in the 3D parallel subspace $E_\parallel^3$, if the m-value corresponds to a crystalline approximant. The value of m can be determined by [18]

$$m = -\frac{\tau - \alpha}{\tau\alpha + 1}$$

where τ is the golden ratio and α is the ratio of the distance between diffraction spots B and C to the distance between diffraction spots A and B, as shown in figures 2(*a*) and 3(*a*). From figures 2(*a*) and 3(*a*), we have measured $\alpha = 1.32$ and hence $m = -0.10$. Obviously, when $\alpha = \tau$, m becomes zero and the phason strain vanishes; when α takes a rational value, all diffraction spots will be arranged periodically along the vertical direction. A particular case is $\alpha = 1$ and hence $m = -0.236$ [18].

Figures 2(*b*) and 3(*b*) show the simulated EDPs of the Mg–Zn–Y–Zr IQC with SI structure corresponding to figures 2(*a*) and 3(*a*), respectively. In these simulated EDPs the area of each circle is proportional to the intensity of the diffraction spot.

4. Conclusion and discussion

By comparing the experimental EDPs with the calculated EDPs in figures 2 and 3, we find good qualitative agreement except for the intensities of some diffraction spots. For instance, spot A in figure 2(*a*) is weaker than its simulation in figure 2(*b*); some spots (shown by arrows) in figure 3(*a*) are weaker than their simulations in figure 3(*b*). These may be explained as follows spot A in figure 2(*a*) has shifted along the zone axis, i.e. spot A has slightly deviated from the zero-order Laue zone and hence is weaker than it should be. The same occurs for the spots (shown by arrows) in figure 3(*a*). From these we can conclude that the distorted SI structure has phason strain not only along $Z_\perp$ (see figure 5) but also along $X_\perp$ and/or $Y_\perp$. From figures 2(*a*) and 3(*a*) we can only measure the phason strain along $Z_\perp$.

In addition, we observed that the distorted FCI structure coexists with the SI IQC in the Mg–Zn–RE alloys. The different compositions may play an important role in forming the two kinds of IQC; more detailed work is needed. This work indicates that phason strain is a general phenomenon for the new stable Mg–Zn–Y–Zr IQCs of both SI structure and FCI structure in our samples; this is due to the frozen phason strain since our specimens have not been annealed in a high-temperature relaxation process.

Acknowledgments

This project was supported by the National Natural Science Foundation of China and the Provincial Natural Science Funds of Henan, People's Republic of China (930404100).

References

[1] Schechtman D, Blech I, Gratias D and Cahn J W 1984 *Phys. Rev. Lett.* **53** 1951
[2] Bendersky L 1985 *Phys. Rev. Lett.* **55** 1461
[3] Ishimasa T, Nissen H-U and Fukano Y 1985 *Phys. Rev. Lett.* **55** 511
[4] Wang N, Chen H and Kuo K H 1987 *Phys. Rev.* **59** 1010
[5] Feng Y C, Lu G, Ye H Q, Kuo K H, Withers R L and Van Tendeloo G 1990 *J. Phys.: Condens. Matter* **2** 9749
[6] Marcus M A and Elser V 1986 *Phil. Mag. Lett.* B **54** L101
[7] Guyot P and Audier M 1987 *Mater. Sci. Forum* **22–4** 247
[8] Yu N, Portier R, Gratias D, Yu-Zhang K and Bigot J 1987 *Mater. Sci. Forum* **22–4** 579
[9] Tasi A P, Inoue A and Masumoto T 1987 *Japan. J. Appl. Phys.* **26** L1505
[10] He L X, Wu Y K and Kuo K H 1990 *Quasicrystals and Incommensurate Structures in Condensed Matter* ed M J Yacaman, D Romeu, V Castano and A Gomez (Singapore: World Scientific) p 372
[11] Grushro B 1992 *Phil. Mag. Lett.* **66** 151
[12] Maamar S and Harmel M 1991 *Phil. Mag. Lett.* **64** 343
[13] Beeli C, Nissen H-U and Robadey J 1991 *Phil. Mag. Lett.* **63** 87
[14] Tsai A P, Inoue A and Masumoto T 1991 *Phil. Mag. Lett.* **64** 163
[15] Ohashi W and Spaepen F 1987 *Nature* **330** 555
[16] Lubensky T C, Socolar J E S, Steinhardt P J, Bancel P A and Heiney P A 1986 *Phil. Mag. Lett.* **57** 1440
[17] Li F H, Teng C M, Huang Z R, Cheng X C and Chen X D 1988 *Phil. Mag. Lett.* **2** 113
[18] Li F H 1993 *Crystal–Quasicrystal Transitions* ed M J Yacaman and M Torres (Amsterdam: Elsevier) p 27
[19] Luo Z, Zhang S, Tang Y and Zhao D 1993 *Scr. Metall.* **28** 1513
[20] Ebalard S and Spaepen F 1989 *J. Mater. Res.* **4** 39
[21] Kramer P 1985 *Z. Naturf.* a **40** 775
[22] Elser V 1986 *Acta Crystallogr.* A **42** 36
[23] Zhao D, Wang R, Cheng Y and Wang Z 1988 *J. Phys. F: Met. Phys.* **18** 1893